2020

Comparison of RANS Turbulence Models in Predicting Wake Development in a 2-Dimensional Actuator Disk Model

Chee Meng Pang
Dundalk Institute of Technology, chee.pang@dkit.ie

David Kennedy
Technological University Dublin, david.kennedy@tudublin.ie

Fergal O'Rourke Dr
Dundalk Institute of Technology, fergal.orourke@dkit.ie

Recommended Citation

Pang, C.E., Kennedy, D. (2020). Comparison of RANS Turbulence Models in Predicting Wake Development in a 2-Dimensional Actuator Disk Model. *33rd International Conference on Efficiency, Cost, Optimization, Simulation and Environmental Impact of Energy Systems (ECOS 2020)*, Osaka, Japan, June 29 - July 3. (conference cancelled due to Covid19 but papers were submitted and peer reviewed). doi:10.21427/hy7w-sm26

Comparison of RANS turbulence models in predicting wake development in a 2-dimensional actuator disk model

Conference Paper · September 2020

CITATIONS
0

READS
91

3 authors:

Chee Meng Pang
Dundalk Institute of Technology
5 PUBLICATIONS **2** CITATIONS
SEE PROFILE

David Kennedy
Technological University Dublin - City Campus
44 PUBLICATIONS **790** CITATIONS
SEE PROFILE

Fergal O'Rourke
Dundalk Institute of Technology
27 PUBLICATIONS **795** CITATIONS
SEE PROFILE

Comparison of RANS turbulence models in predicting wake development in a 2-dimensional actuator disk model

Chee Meng Pang[a], David M. Kennedy[b], Fergal O'Rourke[c]

[a] *Centre for Renewables and Energy at Dundalk Institute of Technology, School of Engineering, Dundalk, Ireland,* *cheemeng.pang@dkit.ie*

[b] *Department of Mechanical Engineering, Technological University Dublin, Dublin 1, Ireland,* *david.kennedy@tudublin.ie*

[c] *Centre for Renewables and Energy at Dundalk Institute of Technology, School of Engineering, Dundalk, Ireland,* *fergal.orourke@dkit.ie*

Abstract:

One of the most popular methodologies used to predict the wake of a tidal stream turbine (TST) is the RANS turbulence models coupled with the actuator disk method. This methodology has been widely adopted in the in the wind industry, since the mid-1990s, to predict wake development of wind turbines. Moreover, the reason for its popularity is its capability to give accurate results at an affordable computational cost, and the application of 2-dimensional actuator disk approach could further reduce the computational cost. In this paper, a number of RANS turbulence models represented by a porous disk were used to simulate the wake development behind a TST, the findings were compared. The models adopted in this work are the Standard k-ε model, the Standard k-ω model, the RNG (Re-Normalised Group) k-ε model, the SST (Shear Stress Transport) k-ω model and the RSM (Reynold Stress Model). The results are also validated against experimental measurements found in literature, with a key focus on comparing the downstream velocity and turbulence intensity. It has shown that the Standard k-ε model is best at predicting downstream wake velocities while the SST k-ω model is better at predicting downstream wake turbulence intensity. Mesh convergence studies were conducted to optimise the computational efficiency for each turbulence model used.

Keywords:

Computational Fluid Dynamics, tidal turbine, wake, tidal energy, actuator disk, RANS.

1. Introduction

Marine tidal currents have some beneficial features over other renewable resources such as high predictability and availability. Tidal cycles are very predictable with time-varying flow and direction, which is ideal for optimised energy output [1,2]. The idea of extracting kinetic energy from marine tidal currents is an old idea and in more recent years, this energy source has seen successful full-scale prototype development and testing with a number of commercial-scale devices in full operation around the globe. For TST technology to attain optimum electricity production on a commercial-scale, turbines have to be installed in arrays to maximise the extractable power [3,4]. The maximum available extractable power was predicted according to the Betz limit. Numerical hydrodynamics models of TST can be used to optimise array arrangement or to assess the performance of the turbines. To determine the optimal TST array layout, several investigations have been undertaken to study the effects of array scale and configuration on the power output. Furthermore, energy extraction using TSTs induces a wake flow which may disturb the downstream tidal current flow and the performance of the downstream TSTs [5]. Thus, it is crucial to develop a computationally efficient model to better understand the effect of a turbine wake on the operation of another turbine placed downstream of the former . Two popular modelling approaches to represent a TST is the Actuator Disk (AD) [6,7,8,9,10] and the Blade Element Momentum (BEM) [11,12,13,14]. In this paper a focus is placed on the AD method, the AD method has been widely used since the mid-1990s and this approach estimates the forces that the turbine exerts on the fluid flow, over a disk that represents the turbine. Thus, with the right turbulence model applied,

significant improvements in computational efficiency can be achieved by reducing the time and computational power needed. The computational cost can be further decreased by simulating the turbine in a 2-dimensional domain instead of a 3-dimensional domain.

There were many existing method to close the Reynolds Averaged Navier Stokes (RANS) equations such as k-ω model, k-ε model, Reynold Stress Model, Detached Eddy Simulation (DES), Large Eddy Simulation (LES), Direct Numerical Simulation (DNS) and more. However, methods like DES, LES and DNS are computationally expensive and therefore their use is limited to solving local scale modelling such as flow around a single turbine or single blade. In contrast, the as k-ω model, k-ε model, and their variant can represent a huge variety of flow at a low affordable computational cost. This is of great importance as the simulation of multiple devices relies on the applicability of the model to deliver a quick and affordable solution. The as k-ω and k-ε model has numerous different types and variants, hence selecting the appropriate model is critical as the model performance varies significantly depending on the flow conditions. In this paper, five popular turbulence models were investigated: the Standard k-ε model, the Standard k-ω model, the RNG (Re-Normalised Group) k-ε model, the SST (Shear Stress Transport) k-ω model and the RSM (Reynold Stress Model). The k-ε model establishes the background for several turbulence models, it is computationally inexpensive and yet provided accurate results and easily implementation [15]. However, the k-ε model is not suitable for complex flows. Whereas, the k-ω model typically predicted to be excessive and early in this application due to separation [16]. The SST k-ω model is a variant k-ω model, it combines both k-ε model and k-ω model which accounts for the transport of turbulent shear stress and gives highly accurate predictions of the onset and the amount of flow separation for an adverse pressure gradient but need mesh refinement close to the wall [17]. The RNG k-ε model is an improved variant of the original k-ε model, it provides an option to account for the effects of swirl or rotation by modifying the turbulent viscosity [18]. However, it is much more difficult to obtain converged results far from the boundary in the free stream region. The RSM is considered the most difficult method to obtain a solution to the RANS equation. Furthermore, it is anisotropic and does not use the Boussinesq assumption. It is great for solving strong swirl, adverse pressure gradients, and anisotropic turbulence, but it is highly complex and has limited success in obtaining accurate results [19]. Importantly, it is also computational costly.

There are three fundamental limitations in the use of steady state RANS-actuator disk models. Firstly, the disk is non-rotating therefore eliminating any swirl in the flow. Beyond the near wake, which is generally beyond 5D downstream, has a similar structure to that of a turbine [20]. Swirl in the near wake can persist further downstream potentially influencing the flow boundaries and cause distortion in the wake [21]. Secondly, it is assumed that tip vortices from a rotating turbine blade are ignored due to the actuator disk's inability to replicate these vortices [22]. Thirdly, transient flow characteristics are not accounted for in the steady-state RANS-actuator disk model. This model provides information about mean flow and assumes isotropic turbulence. Hence, it is useful in understanding the characterises of the flow behind the turbine [23]. Besides modelling the turbulence generated by the turbine, the ambient condition should be understood to better estimate the flow around the turbine to closely match the realistic configuration of a real turbine. Some studies have been undertaken investigating the ambient turbulence effects on the wake characteristics and the flow recovery [10,24]. This is of great importance as a high level of turbulence intensity has been observed at most potential sites for deployment of TST [25,26].

Numerous studies have been carried out on TSTs using the RANS-actuator disk model and the predictions of the velocities and turbulence intensities in the wake [23]. Studies done by Harrison M.E., et al. (2010) from University Southampton [27] and V.T. Nguyen from Hanoi University [8] have highlighted the performance of RANS-actuator disk models in 3-dimensional domains, which show that standard k-ε model performed well in both cases. Hence, in this paper, a computational investigation is conducted on the performance of a RANS-actuator disk model of different turbulence conditions using a 2-dimensional domain and are compared with experimental laboratories data [28] to determine the most suitable turbulence model (the 2-dimensional domain is 3-dimensional but the domain has a thickness of one element). Furthermore, the 2-dimensional

model will also process the solution in a standard unmodified open-flow condition to identify the short-comings of different turbulence models in predicting the wake effects. This methodology is a computational efficient technique that can be used to predict the wake effects of a TST.

2. Theory

2.1. Actuator Disk Theory

The actuator disk (AD) theory is a method used to represent the rotor of the turbine, where a thrust force, F_t, is homogeneously distributed along the disk. The AD has limitations and cannot replicate swirl caused by the rotating turbine rotor in the fluid. However, most swirl components of the flow usually dissipate in the near wake of the turbine (less than 5D downstream of the rotor) and generally plays a less significant role in the far wake of the turbine. Despite the limitations, the AD method has demonstrated an ability to model the far wake condition of the turbine provided that the scale effects are properly parametrised with the suitable production of turbulence.

The introduction of the AD will result in a discontinuity of pressure, a decrease in downstream flow velocity of the rotor and a reduction in kinetic energy of the flow [29]. All these effects are caused by the application of thrust force at the disk area. The thrust force can be calculated using Eq. (1) where ΔP is the difference in pressure before and after the disk, A is the disk area, C_t is the thrust coefficient, ρ is the density of the fluid and U_0 is the upstream flow velocity [20,30]. The thrust coefficient, C_t, is determined by features of the turbine blade such as the pitch of blade, geometry and rotational speed and according to Betz limit, the optimum condition for maximum power output is when the thrust coefficient is equal to 8/9 [31].

$$F_t = \Delta PA = \frac{1}{2} C_t \rho A {U_0}^2 \quad (1)$$

The thrust force,F_t, in Eq. (1) is expressed as a function of the free (upstream) flow velocity [32], this expression works well in predicting the thrust force of a single turbine. However, when analysing an array of turbines the description of a free flow velocity can be unclear and ambiguous. Therefore, it is much preferable to use the local velocity U_d, this is the velocity at where the force was being applied, in this case the disk area. With the consideration of the flow through a porous disk and the use of local velocity, it would be easier to apply a resistance coefficient, *K*, instead of thrust coefficient [33]. Hence, the establishment of Eq. (2) which connects the freestream velocity to local velocity using the resistance coefficient [10]. The resistance coefficient acts as a proportionality coefficient between pressure drop and local velocity squared as shown in Eq. (3). By using Eq. (1) to (3), the relationship between the thrust coefficient and resistance coefficient can be derived as seen in Eq. (4). Hence, by modelling the blade at the optimal condition of C_t= 0.889, the resistance coefficient was determined to be a value of *K = 2*. This value will be used in modelling the porosity characteristic of the actuator disk domain. Lastly, the thrust force is included in the hydrodynamic equation in the form of volumetric force, S_i , this was obtained by dividing the thrust force with the volume of the disk seen in Eq. (5) where *e* is the thickness of the disk.

$$U_0 = U_d \left(1 + \frac{1}{4} K\right) \quad (2)$$

$$\Delta P = \frac{1}{2} \rho K {U_d}^2 \quad (3)$$

$$C_t = \frac{K}{(1+\frac{1}{4}K)^2} \quad (4)$$

$$S_i = \frac{F_t}{Ae} = \frac{1}{2} \rho \frac{K}{e} {U_d}^2 \quad (5)$$

2.2. Reynolds-averaged Navier-Stokes equations

The forces exerted by the actuator disk on the fluid is applied as a source term, S_i, in the RANS equation of momentum conservation in Eq. (6) and solved together with a mass continuity equation seen in Eq. (7) [34]. The source terms are only applied at elements within the actuator disk region.

$$\frac{\partial(\rho U_i U_j)}{\partial x_j} = \frac{\partial P}{\partial x_j} + \frac{\partial}{\partial x_j}\left[\mu\left(\frac{\partial U_i}{\partial x_j} + \frac{\partial U_j}{\partial x_i}\right) + R_{ij}\right] + \rho g_i + S_i \qquad (6)$$

$$\frac{\partial U_i}{\partial x_i} = 0 \qquad (7)$$

Einstein's Notation is used in Eq. (6) and Eq. (7) for brevity. U_i is the time-averaged mean velocity, x_i is the spatial distance, μ is the fluid viscosity, g_i is the component gravitational acceleration and $R_{ij}$is the Reynold stress tensor.

In this paper, five different turbulence models were investigated to close the RANS equation by modelling the Reynolds stresses. These different models were the Standard k-ε model, the Standard k-ω model, the RNG (Re-Normalised Group) k-ε model, the SST (Shear Stress Transport) k-ω model and the RSM (Reynold Stress Model). The Boussinesq assumption was used to solve the equation for all different models expect for RSM. According to the Boussinesq assumption, the Reynold stresses are related to mean flow, turbulence kinetic energy, *k*, and eddy viscosity μ_t as shown in Eq. (8) [35]. Whereas the RSM calculated each term of the Reynolds tensor R_{ij} by using transport equation, the implementation of such method is to avoid the assumption of isotropy.

$$-\rho\overline{u_i' u_j'} = \mu_t\left(\frac{\partial U_i}{\partial x_j} + \frac{\partial U_j}{\partial x_i}\right) - \frac{2}{3}\rho k\delta_{ij} \qquad (8)$$

The Navier Stokes Equations were resolved with CFX™ 19.0. The turbulence and momentum source terms are introduced via the User Defined Function (UDF) of ANSYS CFX [36]. The type of RSM used in this paper was the RSM SSG (Speziale-Sarkar-Gatski) model, this RSM method is a full second-moment Reynolds stress model, which use an omega equation for the length scale equation [37].

3. Methodology

3.1. Experimental Model

The experimental data used to assess the performance of the numerical models was based on the experiment carried by Harrison, M.E., et al. from the University of Southampton [28]. In the experiment conducted, the turbulence intensity was measured along with velocity behind a non-rotating porous disk representing a tidal turbine. The experiment was conducted in a circulating current flume with the dimension of 21m in length and 1.35m in width. The water depth, *H*, was 0.3m [20]. The porous disk used had a diameter of 0.1m and a thickness, *e*, of 0.001m. It is placed at mid-depth and the distance of the disk from inlet and outlet is 20D and 30D respectively. Measurements of the experiment were obtained using Acoustic Doppler Velocimetry with a sampling frequency of 50Hz. It has an accuracy of 1% and the duration of the burst is three minutes each. The mean inlet velocity is 0.3m s^{-1} and the mean inlet turbulent intensity is 5%. The disk has a resistance coefficient *K=2* which corresponds to thrust coefficient C_t= 0.86, based on Betz limit a Ct value close to 0.89 yield a desirable coefficient of power.

3.2. Numerical Model

3.2.1. Porous Disk configuration

The AD domain of 0.1m length and 0.001m thickness was described as a porous domain with 3 main factors influencing its characteristics, these were volume porosity, θ, permeability K_{perm} and resistance loss coefficient K_{loss}. According to Taylor [33], a relationship can be formed between volume porosity, θ, and the resistance coefficient, $K=2$ shown in Eq. (9). This relationship has been examined by Whelan [38] which shows this relationship as a reasonable approximation. The actuator disk applies a resistance to the incoming fluid flow. This resistance causes the actuator disc to experience force similar to that of a turbine operating under the same conditions. Therefore, the porous region is defined with an isotropic loss model where according to Darcy, the flow rate is proportional to a disk's cross-sectional area and pressure drop, but inversely proportional to the thickness. This can be explained using Ergun's equation to determine permeability, K_{perm} [39] shown in Eq. (10). The K_{perm} governs low-speed viscous losses, where D_P is the equivalent spherical diameter of the particle which was assumed to be $D_P = 1\text{x}10^{-9}$m. While, the resistance loss coefficient, K_{loss} governs inertia effects, according to ANSYS CFX guidebook [40] it is defined as the gradient across the disk thickness shown in Eq. (11).

$$\theta^2 = \frac{1}{1+K} \tag{9}$$

$$K_{perm} = \frac{{D_P}^2\theta^3}{(150(1-\theta)^2)} \tag{10}$$

$$K_{loss} = \frac{k}{L} \tag{11}$$

3.2.1. Fluid Domain configuration

The 2-dimensional fluid domain has dimensions of 10m in length, 1.36m in wide and 0.001m-thick. The Top, Bottom and lateral boundaries are defined as symmetry conditions. While the outlet faces were described as opening boundaries with entrainment conditions with zero relative pressure and zero turbulence gradient. The disk is located at mid-depth and the distance of the disk from inlet and outlet is 20D and 30D respectively. The velocity at the inlet boundary was defined as a normal inlet velocity of 0.3m/s with 5% turbulence intensity. The parameter setting of each boundary is summarised in Table 1.

Table 1. Boundaries Condition Parameter

Parameter (Face)	*Setting*
Inlet	Normal inlet speed of 0.3m/s and 5% turbulence intensity
Outlet	Opening entrainment, 0 Pa
Top and Bottom	Symmetry
Lateral	Symmetry

3.2.1. Mesh Convergence Studies

A mesh convergence study was conducted by increasing the number of elements within the computational fluid domains. This was achieved by only increasing the mesh density around the most significant regions of the flow field and leaving the global mesh area unchanged as shown in Fig. 1 [10]. The semicircle of the area of interest has a diameter of 2D and the rectangular area after the disk extended to the outlet. This method significantly reduces the computational requirements needed to solve the simulation by prioritising the area with high-velocity gradients. Three mesh densities were implemented to achieved coarse, medium and fine meshes for a mesh independence study for three different turbulence models which where SST model, Standard k-ε model and RSM.

These studies were conducted on a Dell PC with 16GB RAM and Intel® Core™ i7-8700 3.20 GHz processor and the solver were run on 4 parallel platform to further reduce the computational time.

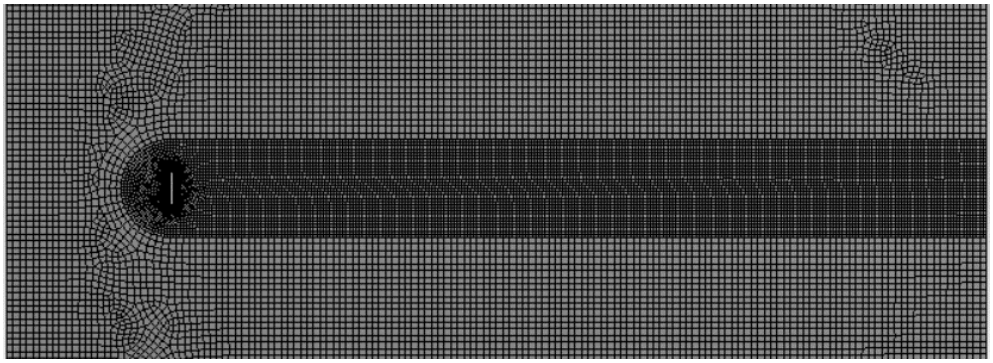

Fig. 1. Computational mesh showing high-density mesh in the actuator disk region and the wake downstream of the actuator disk.

The mesh independence study was done with maximum residuals of 1 $x10^{-6}$ and was allow to run until the solution is converge. The variation in the number of elements occur in the region of interest needed for this study as seen in Fig.1 is achieved by decreasing the size of the element by a factor of 2 and thus produce a higher number of elements and nodes. Table 2 gives details on the mesh convergence studies for each of the turbulence models and the computational time requirements. Among all three turbulence models compared, the RSM model was the most computational expensive as it required more time to solve the Reynolds stresses. Whereas when comparing both SST model and Standard k-ε model, both used roughly the same amount of time to solve in most cases and the changes in term of downstream velocity is not significant as compare to RSM model, this is further observed in Fig.2.

Table 2. Effects of the increasing number of Elements on downstream centreline velocity.

Turbulence Model	*No. of elements*	*No. of nodes*	*Normalised velocity at downstream*					*Solver Time (hrs: min: sec)*
			4D	*7D*	*11D*	*15D*	*20D*	
k-ε model	$3.55\ x10^4$	$4.18x10^4$	0.049	0.513	0.763	0.846	0.896	00:28:09
k-ε model	$1.03x10^5$	$1.19x10^5$	0.542	0.725	0.829	0.892	0.933	01:15:29
k-ε model	$3.69x10^6$	$4.15x10^6$	0.553	0.74	0.846	0.91	0.952	04:57:48
SST model	$3.55\ x10^4$	$4.18x10^4$	0.467	0.688	0.808	0.871	0.925	00:28:22
SST model	$1.03x10^5$	$1.19x10^5$	0.621	0.776	0.871	0.921	0.967	01:14:48
SST model	$3.69x10^6$	$4.15x10^6$	0.403	0.696	0.854	0.929	0.983	03:57:43
RSM model	$3.55\ x10^4$	$4.18x10^4$	0.423	0.567	0.66	0.71	0.747	00:43:11
RSM model	$1.03x10^5$	$1.19x10^5$	0.529	0.708	0.825	0.888	0.933	02:50:34
RSM model	$3.69x10^6$	$4.15x10^6$	0.534	0.715	0.833	0.896	0.943	08:24:21

The turbulence intensity and velocity profile in the k-ε and SST model showed very little changes when the number of elements increased above $1.03x10^6$, suggesting that both of these models don't need a dense mesh to obtain accurate results. A medium-density with $1.03x10^6$ elements was sufficient in both the k-ε model and SST model with a computational solving time of 1 hour 15 minutes and 1 hour 14 minutes respectively. This mesh configuration is also applied in both the RNG k-ε model and standard k-ω model since the RNG model is a variant of the standard k-ε model and SST model is a variant of the standard k-ω model. The RSM (SSG) model needed a more dense mesh and a high number of elements in predicting the turbulence intensity profile to obtain accurate results as seen in Fig. 2f, the RSM (SSG) needed number of elements above $3.69x10^6$ to showed results closely matching the experimental results. While the velocity profile of RSM (SSG) model converged above $1.03x10^6$ number of elements. Hence the time taken to obtain a

high-density mesh solution for RSM (SSG) model was 8 hours 24 minutes. This model was the least computationally efficient.

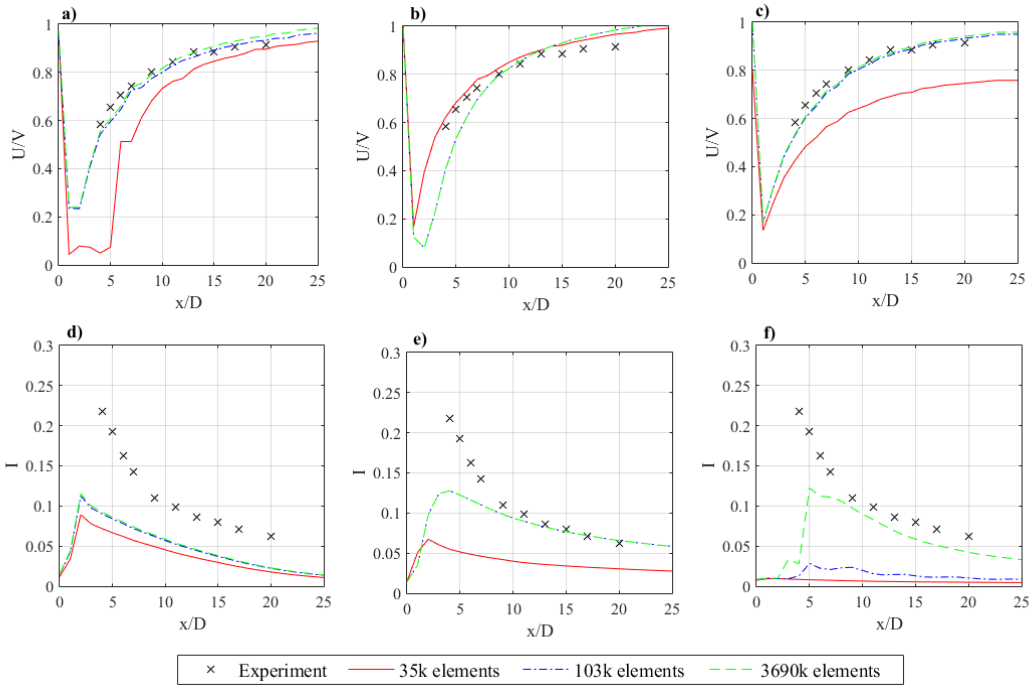

Fig. 2. Effect of changing number of elements on normalised velocity, U/V (where V is the upstream velocity): a) k-ε model, b) SST model and c)RSM SSG;and downstream turbulence intensity, I: d) k-ε model, e) SST model and f) RSM SSG, along the disk centreline axis (x=0 is the disk position) in comparison to experimental results [28].

4. Results

The performance and results of the 2-dimensional actuator disk model using a number of different turbulence models were assessed by comparing with measured experimental results carried by Harrison from the University of Southampton [28]. The focus of this work is on comparing the downstream tidal current velocity and turbulence intensity from the experimental data with the numerical model findings presented in this paper. The comparison was done by comparing the distribution along the horizontal axis, as shown in Fig.3 and on the vertical distribution, shown in Fig.4, downstream from the disk.

The comparison has indicated a strong correlation when comparing between the experiment result and the five turbulence model in terms of velocity distribution downstream as shown in Fig. 3a. However, all five turbulence model shows poor correlations with the experimental measurements in term of turbulence intensity and was under-predicting before D10 as shown in Fig. 3b. When comparing the downstream velocity profile, it was noticed that the k-ε model, RNG k-ε model and RSM (SSG) slightly under-predicted the downstream velocity recovery up until D15 while SST k-ω model slightly over-predicted the velocity recovery as shown in Fig. 3 and Fig. 4. Furthermore, only k-ω model shows to be closely matching the experimental result in term of velocity up until D15. However, after D15 all 5 models were observed to be slightly over-predicting the downstream velocity recovery as shown in Fig. 4. When comparing the downstream turbulence profile, it was noticed that k-ε model and RSM (SSG) model show sign of underestimation in turbulence. Furthermore, the k-ω, SST k-ω and RNG k-ε model underpredict before D10, however after D10 all three model overpredict the turbulence intensity as seen in Fig. 4.The accuracy of the model can be further investigated by carrying out statistical analysis to determine the root mean square error (RMSE) and mean absolute percentage error (MAPE). RSME and MAPE can indicate how well the numerical model, and turbulence models, correlates to the measured data as seen in Table. 3.

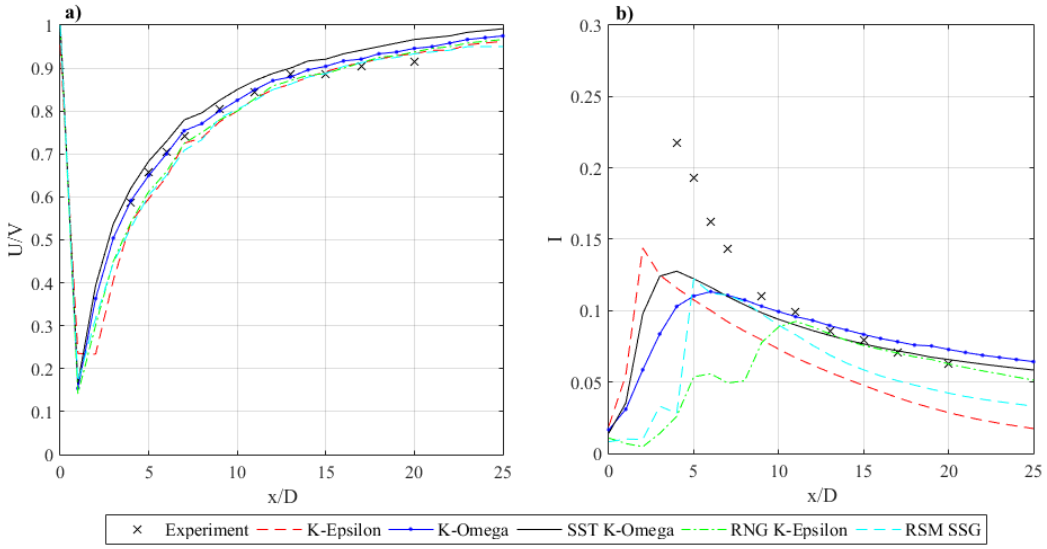

Fig. 3. The downstream centreline normalised velocity: a) normalised velocity, U/V (where V is the upstream velocity) and downstream turbulence intensity: b) turbulence intensity, along the disk centreline axis (x=0 is the disk position) in comparison to experimental results [28].

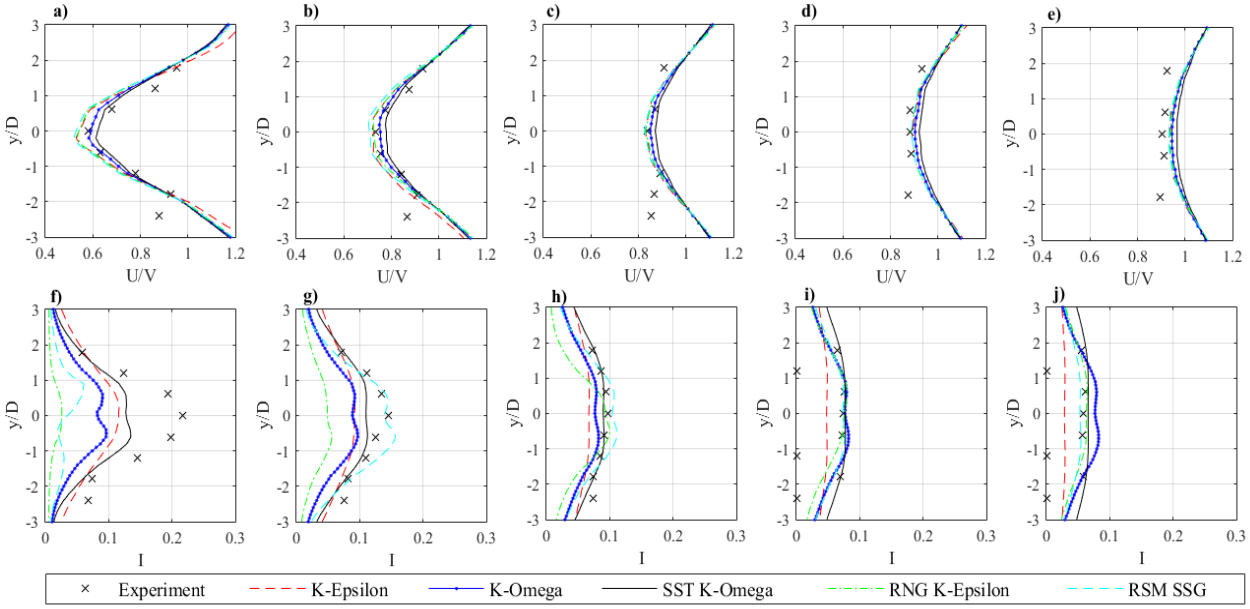

Fig. 4. Downstream vertical profile of axial normalised velocity: a) 4D, b) 7D, c) 11D, d) 15D and e)20D; and turbulence intensity: f) 4D, g) 7D, h) 11D, i) 15D and j) 20D from the disk (y=0 is the centre axis position of the disk) in comparison to experimental results [28].

The standard k-ω model has the closest correlation with the measured data in term of velocity, with an RSME and MAPE of 0.014 and 1% respectively, while the SST k-ω model correlates closest with the measured data in terms of turbulence intensity with RSME and MAPE values of 0.026 and 19% respectively. In contrast, the RSM (SSG) model shows the least correlation with the measured data with velocity and the RNG k-ε model shows the least correlation with the measured data with turbulence intensity. When observing RSME and MAPE in term of velocity, the most suitable is the Standard k-ω model followed by RNG k-ε, then SST k-ω model, and lastly is the Standard k-ε model and RSM (SSG) model. Whereas when observing RSME and MAPE in term of turbulence intensity, the most suitable is the SST k-ω model, followed by Standard k-ω, then RSM (SSG) models, and lastly are the Standard k-ε model and RNG k-ε model. Table 3 also shows that the 2-dimensional actuator disk model exhibits a huge problem in

accurately predicting turbulence intensity with all turbulence models showing huge MAPE values ranging from 40% up to 93%. Hence, the optimum best selection turbulence model for running a 2-dimensional actuator disk problem is either the SST k-ω model or the Standard k-ε model. Further comparison can be undertaken by comparing the contour plot of different models in terms of velocity and turbulence kinetic energy (TKE), shown in Fig. 5 and 6.

Table 3. Root mean square error (RSME) and mean absolute percentage error (MAPE) of velocity and turbulence intensity on different turbulence model in comparison to the experimental data.

Model	*S*tandard *k-ε*	*S*tandard *k-ω*	*SST k-ω*	*RNG k-ε*	*RSM (SSG)*
RSME $_{Velocity}$	0.033	0.014	0.033	0.028	0.034
MAPE $_{Velocity}$ (%)	4	1	4	3	4
RSME $_{Turbulence}$	0.055	0.049	0.026	0.088	0.060
MAPE $_{Turbulence}$ (%)	40	19	19	34	17

When comparing the contour plots of different turbulence models in term of velocity and turbulence kinetic energy (TKE), some apparent differences and similarity are observed between the models shown in figure 5 and 6. The is little difference in the velocity contour between all five difference model. Whereas, huge different was observed in TKE contour between the five models. As seem in Fig 6d and 6e, both the RNG k-ε and RSM (SSG) model were clearly underpredict in the near wake region. The difference in the shape of TKE contour could be caused by turbulence mixing from the surrounding ambient conditions, it is observed that turbulence mixing occurs in the near wake area which might have caused the turbulence kinetic energy to dissipate earlier around the vicinity of the disk as seen in Fig. 5. Furthermore, this could affect the velocity recovery downstream of the disk [41], in most cases, the introduction of increased turbulence intensity around the disk would greatly aid in wake recovery [42] but such characteristics were not observed hence further investigation is needed. Another issue observed is due to the nature of the 2-dimensional model, TKE performance might be hindered due to the fact that unlike the 3-dimensional model which experience upstream velocity from the surrounding vicinity circumference of the disk. The 2-dimensional model only experiences upstream velocity from the side of the disk, this may have affected wake recovery. It has found that the downstream velocity had a close-linked to the permeability of the disk and the downstream turbulence intensity had a close-linked to the resistance loss coefficient of the disk. Hence, further study is needed in determine this relationship and improve the performance of downstream turbulence intensity.

4. Conclusion

This paper details the performance of various RANS turbulence models in predicting the wake of a tidal steam turbine in a 2-dimensional domain. Under a standard open flow configuration, it was shown that the SST k-ω model was the optimum selection for predicting both velocity and turbulence intensity. However, for downstream velocity, the standard k-ω model performed the best. The RSM model was overly computational inefficient and time-consuming to implement and it required a highly refined mesh to get desirable results. Further work is needed to investigate the conditions and configurations affecting the performance of various RANS models in 2-dimensional actuator disk problems. Such studies include the introduction of source terms at the disk to account for the underprediction of turbulence intensity downstream, rate of dissipation in turbulence effects on wake recovery, effects of changing permeability and loss coefficient on model accuracy. Further work will also involve comparisons with 3-dimensional actuator disk model representations of a tidal stream turbine operating in tidal flows.

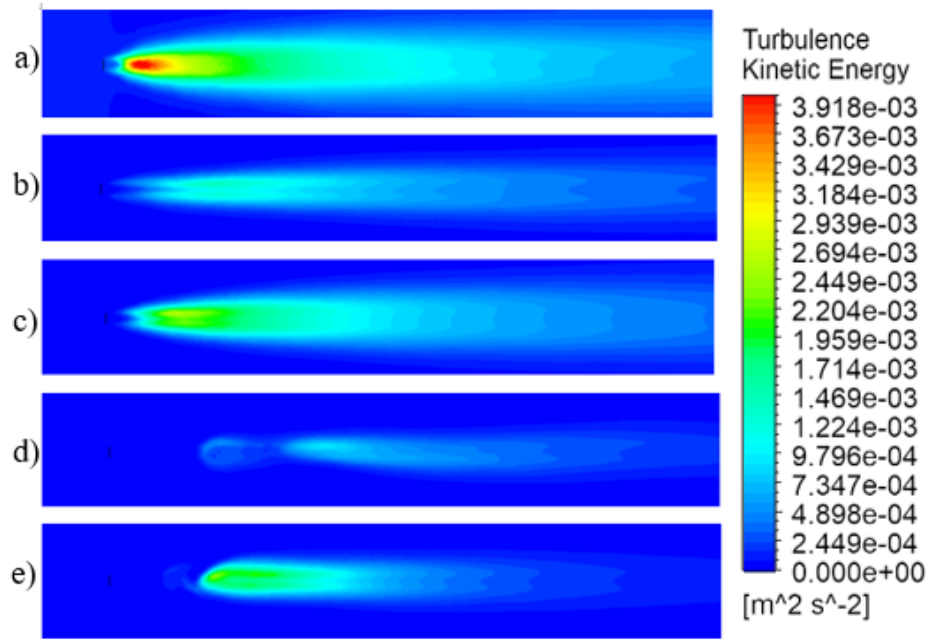

Fig. 5. The contour of turbulent kinetic energy for five different turbulence models: a) Standard k-ε, b) Standard k-ω, c) SST k-ω, d) RNG k-ε model, and e) RSM (SSG).

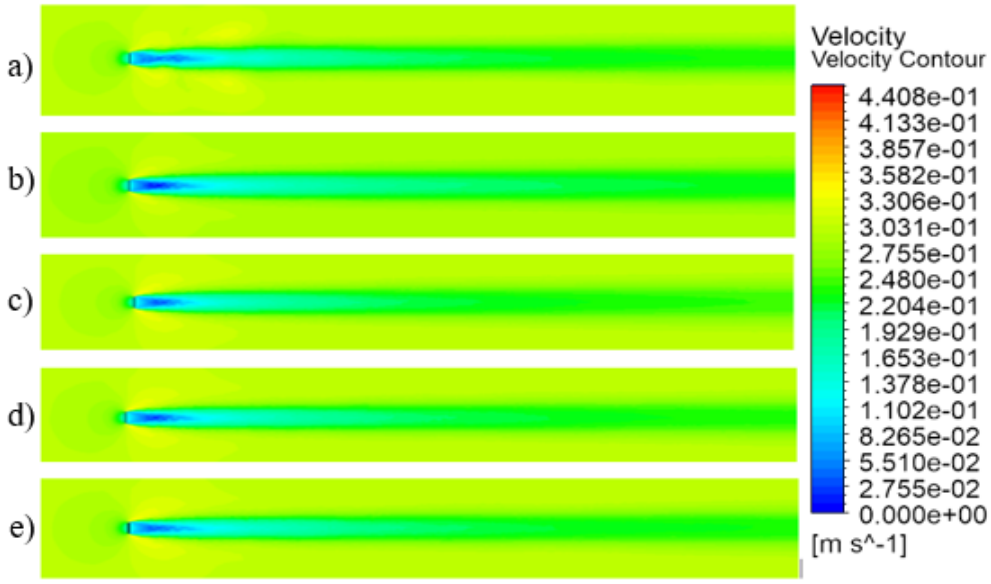

Fig. 6. The contour of velocity for five different turbulence models: a) Standard k-ε, b) Standard k-ω, c) SST k-ω, d) RNG k-ε model, and e) RSM (SSG).

5. References

[1] F. O'Rourke, F. Boyle, and A. Reynolds, "Tidal current energy resource assessment in Ireland: Current status and future update," *Renew. Sustain. Energy Rev.*, vol. 14, no. 9, pp. 3206–3212, 2010.

[2] J. A. Clarke, G. Connor, A. D. Grant, and C. M. Johnstone, "Regulating the output characteristics of tidal current power stations to facilitate better base load matching over the lunar cycle," *Renew. Energy*, vol. 31, no. 2, pp. 173–180, 2006.

[3] R. Vennell, "Exceeding the Betz limit with tidal turbines," *Renew. Energy*, vol. 55, pp. 277–285, 2013.

[4] Y. Chen, B. Lin, J. Lin, and S. Wang, “Experimental study of wake structure behind a horizontal axis tidal stream turbine,” *Appl. Energy*, vol. 196, pp. 82–96, 2017.

[5] B. Morandi, F. Di Felice, M. Costanzo, G. P. Romano, D. Dhomé, and J. C. Allo, “Experimental investigation of the near wake of a horizontal axis tidal current turbine,” *Int. J. Mar. Energy*, vol. 14, pp. 229–247, 2016.

[6] L. Bai, R. R. G. Spence, and G. Dudziak, “Investigation of the Influence of Array Arrangement and Spacing on Tidal Energy Converter (TEC) Performance using a 3-Dimensional CFD Model,” *Proc. 8th Eur. Wave Tidal Energy Conf. Uppsala, Sweeden*, pp. 654–660, 2009.

[7] G. Crasto, A. R. Gravdahl, F. Castellani, and E. Piccioni, “Wake modeling with the actuator Disc concept,” *Energy Procedia*, vol. 24, no. January, pp. 385–392, 2012.

[8] V. T. Nguyen, S. S. Guillou, J. Thiébot, and A. Santa Cruz, “Modelling turbulence with an Actuator Disk representing a tidal turbine,” *Renew. Energy*, vol. 97, pp. 625–635, 2016.

[9] T. Roc, D. C. Conley, and D. Greaves, “Methodology for tidal turbine representation in ocean circulation model,” *Renew. Energy*, vol. 51, pp. 448–464, Mar. 2013.

[10] C. M. Pang, F. O. Rourke, and D. Kennedy, “The Effects of Inflow Turbulence Intensity on predicting wake velocity in a two dimensional RANS Actuator disc model,” *EWTEC 2019*, no. September, 2019.

[11] G. Bai, J. Li, P. Fan, and G. Li, “Numerical investigations of the effects of different arrays on power extractions of horizontal axis tidal current turbines,” *Renew. Energy*, vol. 53, pp. 180–186, May 2013.

[12] J. Bretheim and E. Bardy, “A Review of Power-Generating Turbomachines,” no. April, 2015.

[13] S. R. Turnock, A. B. Phillips, J. Banks, and R. Nicholls-Lee, “Modelling tidal current turbine wakes using a coupled RANS-BEMT approach as a tool for analysing power capture of arrays of turbines,” *Ocean Eng.*, vol. 38, no. 11–12, pp. 1300–1307, Aug. 2011.

[14] I. Ammara, C. Leclerc, and C. Masson, “A viscous three-dimensional differential/actuator-disk method for the aerodynamic analysis of wind farms,” *J. Sol. Energy Eng. Trans. ASME*, vol. 124, no. 4, pp. 345–356, Nov. 2002.

[15] B. E. Launder and D. B. Spalding, “The numerical computation of turbulent flows,” *Comput. Methods Appl. Mech. Eng.*, vol. 3, no. 2, pp. 269–289, 1974.

[16] P. A. Durbin and B. A. P. Reif, *Statistical Theory and Modeling for Turbulent Flows: Second Edition*. John Wiley and Sons, 2010.

[17] F. R. Menter, “Two-equation eddy-viscosity turbulence models for engineering applications,” *AIAA J.*, vol. 32, no. 8, pp. 1598–1605, 1994.

[18] V. Yakhot and S. A. Orszag, “Renormalization group analysis of turbulence. I. Basic theory,” *J. Sci. Comput.*, vol. 1, no. 1, pp. 3–51, Mar. 1986.

[19] C. D. Argyropoulos and N. C. Markatos, “Recent advances on the numerical modelling of turbulent flows,” *Applied Mathematical Modelling*, vol. 39, no. 2. Elsevier Inc., pp. 693–732, 2015.

[20] L. E. Myers and A. S. Bahaj, “Experimental analysis of the flow field around horizontal axis tidal turbines by use of scale mesh disk rotor simulators,” *Ocean Eng.*, vol. 37, no. 2–3, pp. 218–227, 2010.

[21] N. Troldborg, J. N. Sørensen, and R. Mikkelsen, “Actuator line simulation of wake of wind turbine operating in turbulent inflow,” *J. Phys. Conf. Ser.*, vol. 75, no. 1, 2007.

[22] R. Mikkelsen, *Actuator disc methods applied to wind turbines*. 2003.

[23] W. M. J. Batten, M. E. Harrison, and A. S. Bahaj, “The accuracy of the actuator disc-RANS approach for predicting the performance and far wake of a horizontal axis tidal stream

turbine," *Philos. Trans. R. Soc. London A Math. Phys. Eng. Sci.*, vol. 371, no. 1985, 2013.

[24] F. Maganga, G. Germain, J. King, G. Pinon, and E. Rivoalen, "Experimental characterisation of flow effects on marine current turbine behaviour and on its wake properties," *IET Renew. Power Gener.*, vol. 4, no. 6, pp. 498–509, Nov. 2010.

[25] Y. Li, N. Kelley, B. Jonkman, J. A. Colby, R. Thresher, and S. Hughes, "Inflow measurement in a tidal strait for deploying tidal current turbines-lessons, opportunities and challenges," in *Proceedings of the International Conference on Offshore Mechanics and Arctic Engineering - OMAE*, 2010, vol. 3, pp. 569–576.

[26] I. A. Milne, R. N. Sharma, R. G. J. Flay, and S. Bickerton, "Characteristics of the turbulence in the flow at a tidal stream power site," *Philos. Trans. R. Soc. A Math. Phys. Eng. Sci.*, vol. 371, no. 1985, Feb. 2013.

[27] M. E. Harrison, W. M. J. Batten, L. E. Myers, and A. S. Bahaj, "A comparison between CFD simulations and experiments for predicting the far wake of horizontal axis tidal turbines," *Renew. Power Gener.*, vol. 4, no. 6, pp. 613–627, 2010.

[28] M. E. Harrison, W. M. J. Batten, L. E. Myers, and A. S. Bahaj, "Comparison between CFD simulations and experiments for predicting the far wake of horizontal axis tidal turbines," *IET Renew. Power Gener.*, vol. 4, no. 6, pp. 613–627, 2010.

[29] A. M. Biadgo, A. Simonović, D. Komarov, and S. Stupar, "Numerical and analytical investigation of vertical axis wind turbine," *FME Trans.*, vol. 41, no. 1, pp. 49–58, 2013.

[30] F. Castellani and A. Vignaroli, "An application of the actuator disc model for wind turbine wakes calculations," *Appl. Energy*, vol. 101, pp. 432–440, 2013.

[31] A. Rachman and U. Haluoleo, "Exploring the Flow Expansion Causing the Betz Limit Using the Actuator Disk Theory," no. July, 2015.

[32] T. Letcher, *Wind Energy Engineering, 1st Edition, A Handbook for Onshore and Offshore Wind Turbines*. Academic Press, 2017.

[33] G. I. Taylor, *The Scientific Papers of Sir Geoffrey Ingram Taylor*. Cambridge University Press, 1963.

[34] T. J. Chung, *Computational fluid dynamics, second edition*, vol. 9780521769. 2010.

[35] A. A. Shirgaonkar and S. K. Lele, "On the extension of the Boussinesq approximation for inertia dominated flows," *Phys. Fluids*, vol. 18, no. 6, 2006.

[36] T. D. Canonsburg, "ANSYS CFX-Pre User ' s Guide," vol. 15317, no. November, pp. 724–746, 2011.

[37] F. Billard, T. Craft, and A. Revell, "Application of advanced Reynolds Stress Transport Models to highly separated flows," *7th Int. Symp. Turbul. Shear Flow Phenomena, TSFP 2011*, vol. 2011-July, no. July, 2011.

[38] J. Whelan, M. Thomson, J. M. R. Graham, and J. Peiro, "Modelling of free surface proximity and wave induced velocities around a horizontal axis tidal stream turbine," *Proc. 7th Eur. Wave Tidal Energy Conf. Porto Port.*, no. October, pp. 11–14, 2007.

[39] J. P. du Plessis and S. Woudberg, "Pore-scale derivation of the Ergun equation to enhance its adaptability and generalization," *Chem. Eng. Sci.*, vol. 63, no. 9, pp. 2576–2586, 2008.

[40] ANSYS, *Ansys Release 5.6 Manual: Theory Reference*, Eleventh. Canonsburg, PA: ANSYS Inc., 1999.

[41] H. Ren, X. Zhang, S. Kang, and S. Liang, "Actuator disc approach of wind turbinewake simulation considering balance of turbulence kinetic energy," *Energies*, vol. 12, no. 1, 2019.

[42] P. Mycek, B. Gaurier, G. Germain, G. Pinon, and E. Rivoalen, "Experimental study of the turbulence intensity effects on marine current turbines behaviour. Part II: Two interacting turbines," *Renew. Energy*, vol. 68, no. June, pp. 876–892, 2014.